

# We are IntechOpen, the world's leading publisher of Open Access books Built by scientists, for scientists

6,900

Open access books available

185,000

International authors and editors

200M

Downloads

Our authors are among the

154

Countries delivered to

TOP 1%

most cited scientists

12.2%

Contributors from top 500 universities



WEB OF SCIENCE™

Selection of our books indexed in the Book Citation Index  
in Web of Science™ Core Collection (BKCI)

Interested in publishing with us?  
Contact [book.department@intechopen.com](mailto:book.department@intechopen.com)

Numbers displayed above are based on latest data collected.  
For more information visit [www.intechopen.com](http://www.intechopen.com)



# AFM Measurements to Investigate Particulates and Their Interactions with Biological Macromolecules

L. Latterini and L. Tarpani

*Department of Chemistry, Center of Excellence for Nanostructured and Innovative Materials, University of Perugia  
Italy*

## 1. Introduction

In recent years much attention has been paid to the development of metrology methods to investigate particulate matter and its interaction with bio-molecules. This interest is triggered by the potential applications of nanoparticle-biomolecule hybrid systems in different areas such as bio-sensing, catalysis, target delivery, selective recognition, etc. (Amelia et al., 2010; Bellezza et al., 2009; Latterini & Amelia, 2009; Joralemon et al., 2005; Nehilla et al., 2005; Rosi & Mirkin, 2005). Furthermore, a better understanding of the interactions between particles and biomolecules could help to optimize the ability to reduce the exposure to particulate matter in working environments.

In the last decade AFM methods based on a vibrating tip to explore a surface topography experienced a significant transformation which allowed them to reach nm-resolution imaging and become sensitive tools to investigate tip-sample interactions down to sub-nm resolution (García & Pérez, 2002). Hence the chance is to develop quantitative procedures to study material properties with high spatial resolution even without affecting the softest samples. These achievements have shown that AFM methods can be used as a valid alternative to other well established techniques (such as electron microscopies) in the study of nanostructured materials. The good spatial resolution of AFM measurements can be achieved without any sample pre-treatments thus overcoming the limitations in the sample preparation involved in electron microscopies. AFM imaging appears particularly attractive to characterize particulate matter based on organic materials with high spatial resolution without any concerns about scattering cross sections and sample treatment procedures. Extremely interesting in this context is the possibility to use AFM to characterize particles conjugated to biological macromolecules. Indeed, AFM scanning showed a good accuracy to obtain size distributions for colloidal particle samples comparable to dynamic light scattering techniques or even better if the samples were polydispersed (Hoo et al., 2008)

In the present contribution, particulate matter, either intentionally prepared with designed dimensional, morphological and chemical properties or produced in working environments during the phases of metal processing or combustion processes, were dimensionally characterized and information on their surface morphology were obtained.

The characterization of particulates or colloidal nanoparticles in the presence of protein was used to obtain valuable information on the nanoparticle-protein interactions and eventually on the disposition of the macromolecules with respect to the particles. The presented results will be discussed in terms of experimental conditions to enhance or to quench the particulate-biomolecule interaction in order to control the stability of hybrid materials.

## 2. Results

Wet chemical synthesis for colloidal nanoparticle preparation have recently attracted much attention with the aim to optimize the procedures to work in mild conditions (atmospheric pressure, temperature below 100°C); in these conditions, the colloidal samples can be easily characterized by polydisperse size distributions and non-homogeneous shapes. AFM imaging can provide a fast investigation tool to characterize nanoparticle preparations without a prior knowledge of the size distributions and shape. Furthermore, the acquisition of AFM data can give valuable information on the thickness of the stabilizer shell, which has to be necessarily used to control the nanoparticle growth in solution and it is worth to be taken into account as particle constituent. For nanomaterials, the size distribution, surface area, shape, aggregation state and composition strongly affect their biological activity since these properties have an influence on their interactions with biomolecules. AFM in tapping mode has been used to study nanoparticles deposited on mica and to investigate their interactions with proteins and DNA.

### 2.1 Dimensional characterization of colloidal nanoparticles and particulates

AFM topography imaging was helpful to obtain information on the growth mechanism of CdS nanocrystals prepared in water by thermolysis of a single precursor ((2,2'-bpy)Cd(SC{O}Ph<sub>2</sub>)) and the thioglycerol at a constant molar ratio of 1:2.5 and at different refluxing times (from 30' to 5 hours). In particular, the size distribution in the different samples was monitored by AFM measurements. In Figure 1, AFM images recorded on the samples with shortest and longest reaction times, respectively, are reported together with the related size distribution analysis, based on gaussian functions. For the sample refluxed for 30', an average size of  $2.2 \pm 0.1$  nm was determined. On the other hand, for the sample obtained with longer refluxing times, the size distribution appears more complex and two populations can be found: the first with the average size centered at  $3.1 \pm 0.1$  nm and the second (although with lower frequency) having the mean diameter at  $4.8 \pm 0.3$  nm. The size distribution analysis confirmed that the nanocrystal dimensions increased with the refluxing time and underlined that different populations are formed during the nanocrystal growth. In fact, the size histograms showed that, during the growth, the mean diameter increased together with an impressive change in the distribution width. The sample obtained after 30' refluxing presented a broad size distribution (width 2.2 nm), while in the sample obtained with longer refluxing times the most frequent distribution becomes much narrower (width 1.2 nm) and a very broad nanocrystal population (width 6.3 nm) appeared. Since the samples were obtained from the same preparation procedure and contained the same capping agent concentration, the dimension change cannot be attributed to a stabilizer effect. This behaviour can be explained considering that the nanocrystal growth is controlled by surface processes. Most likely the growth is because

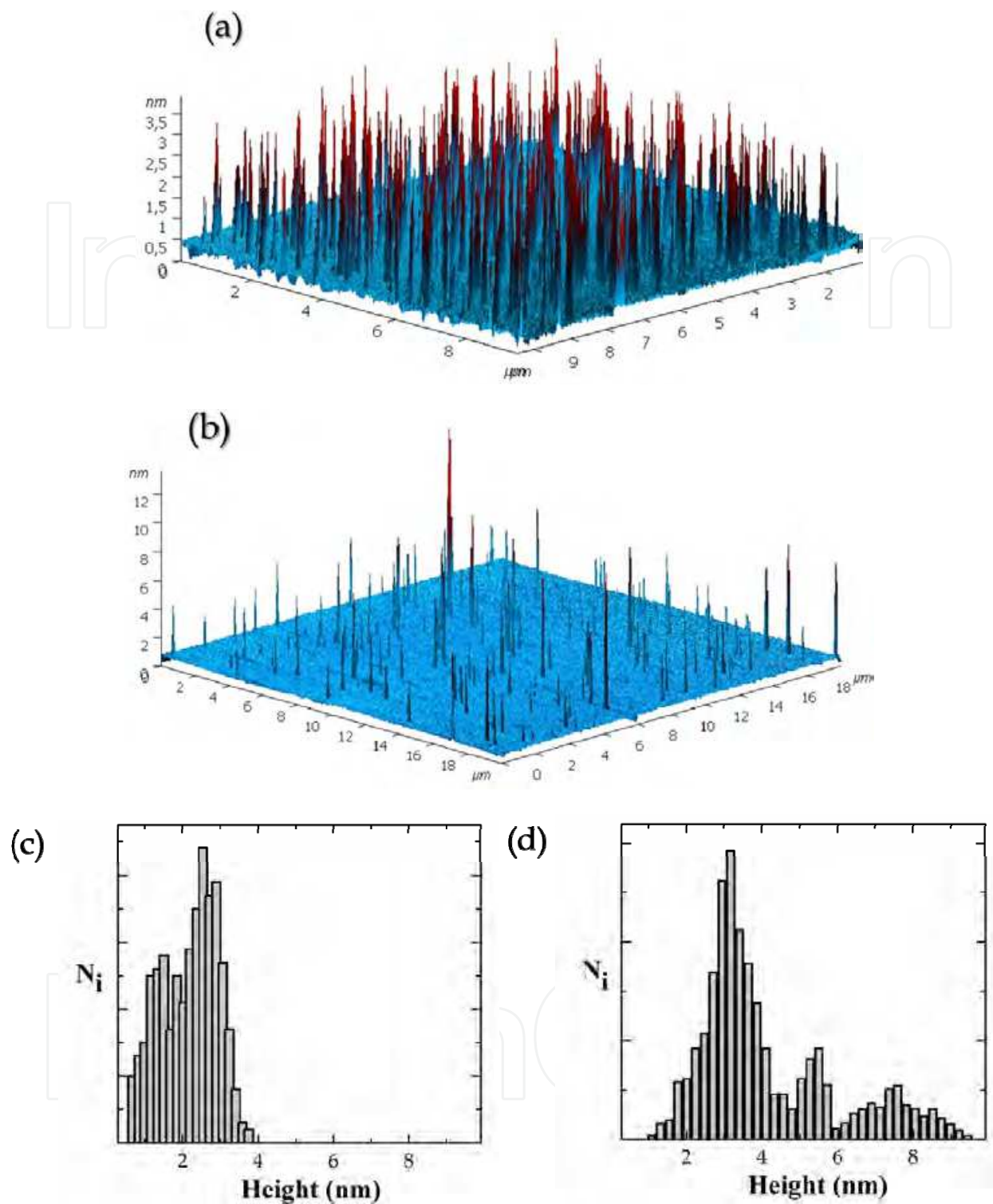


Fig. 1. 3-D topography images of CdS nanocrystal refluxed with thioglycerol for 30' (a) and 5 hours (b) together with their relative height distributions (c, d respectively)

the diffusion of the seeds on the nuclei surface is quite rapid, and therefore it leads to a very broad size. Furthermore, the difficulties to control the growth lead to the development of defects in the crystal structures as confirmed by luminescence studies which show trap states emission (Latterini & Amelia, 2009).

In the case of metal nanoparticles suspensions, the comparison between topography and phase images allowed us to make the hypothesis that the stabilizer shell dimensions cannot be neglected. Gold nanoparticles were prepared in water upon in-situ reduction of Au(III) by citrate anions, which play the double role of reduction agent and stabilizer. AFM images showed isolated nanoparticles with a spherical shape (Figure 2a). The phase images (Figure 2b), recorded simultaneously with the topography images, have shown different contrast for every single grain; indeed a brighter spot corresponding to a higher oscillation phase was observed inside every grain in the phase imaging mode. Similar differences in contrast were not observed in the topography images, suggesting that the grain is actually a nanocomposite material having components which interact differently with the AFM tip. Thus a hypothesis was made that in the chemical composition of colloidal nanoparticles an important component is the organic stabilizer. This hypothesis was further supported by TEM images and from the comparison between AFM and TEM size distribution, an estimate of the stabilizer shell thickness of few nm, depending on the experimental conditions during the synthesis, can be obtained.

In order to explore the effect of citrate ion concentration on the properties of particles, preparations were carried out keeping constant the Au(III) amount and reducing to one half the citrate concentration. AFM images indicated that with lower citrate concentrations the average particles size was smaller ( $12 \pm 0.3$  nm compared to  $20 \pm 0.2$  nm obtained by doubling the citrate content) and the distribution of the dimensions was narrower. These observations indicated that the increase of citrate concentration induced a faster and more efficient nucleation process and allowed better control of the particle growth through a diffusion controlled process, although a thickening of the stabilizer shell cannot be excluded.

Silica nanoparticles prepared via the Stöber method could be easily visualized and characterized through AFM scanning, once the suspension was spin-coated on a mica support (Figure 3a). AFM acquisitions show the spherical shape of the nanoparticles with an averaged diameter of 70 nm as a result of a quite narrow distribution. Additionally, the nanoparticle surface appeared regular and without roughness (Figure 3b). The lack of observing pores on the nanoparticle surface by AFM scanning was most likely because the cavities are smaller than the AFM tips (about 1 nm). Generally the void particles appear well separated on mica, indicating that the surface charges act as efficient capping agents. When the silica particle surface is covalently functionalized with organic dyes, such as fluorescein or 9-aminoacridine, the particle height resulted increased by a factor of two or three (Figure 3c) and the grains do not appear isolated any more, as already observed for similar systems (Latterini & Amelia, 2009). These morphology changes were attributed to the presence of the aromatic dye molecules on the particle surface which reduce the net charge and are able to form aggregate species stabilized by  $\pi$ - $\pi$  stacking. The occurrence of these aggregate species might strongly be reduced in suspension samples for the presence of solvation interactions, but they are predominant in solid state and can strongly affect the chemical-physical behaviour of the samples. Thus attention should be paid in the detection of these aggregated species when devices are prepared from suspensions. AFM is one of the few methods which allows one to visualize the formation of these assemblies.

The particulates produced in working environments during material processing were collected through a standard device which was designed to collect and separate aerosol through dimensional properties. Briefly, a Sioutas Cascade Impactor provides a five step



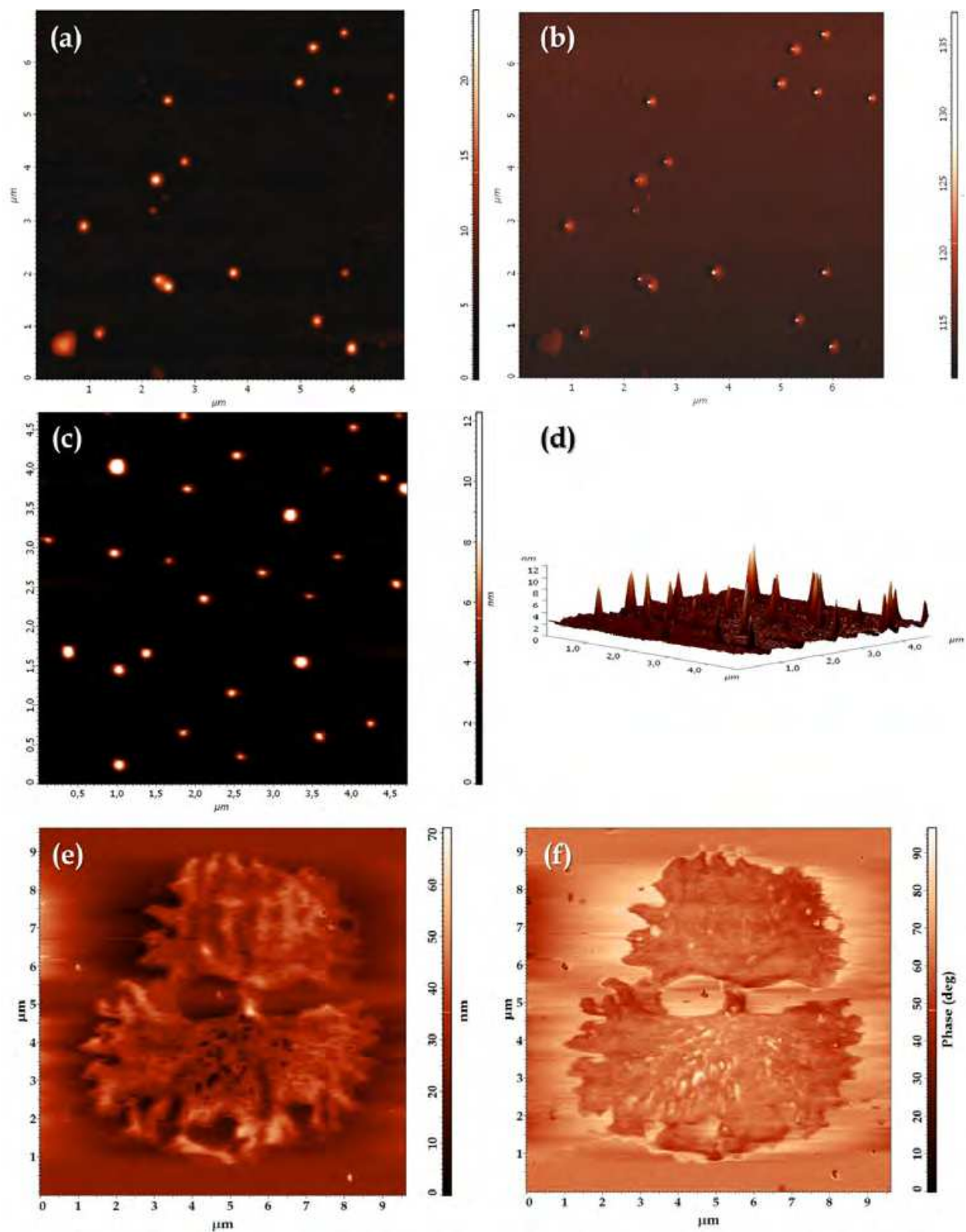


Fig. 2. (upper panel) AFM images in topography (a) and phase (b) mode of gold nanoparticles stabilized by citrate cations prepared with  $[Au(III)]/[citrate]$  of 1:14; (middle panel) 2-D (c) and 3-D (d) topography images of gold nanoparticles prepared with  $[Au(III)]/[citrate]$  of 1:7; (lower panel) AFM images in topography (e) and phase (f) of gold nanoparticles upon interaction with bacterial DNA.

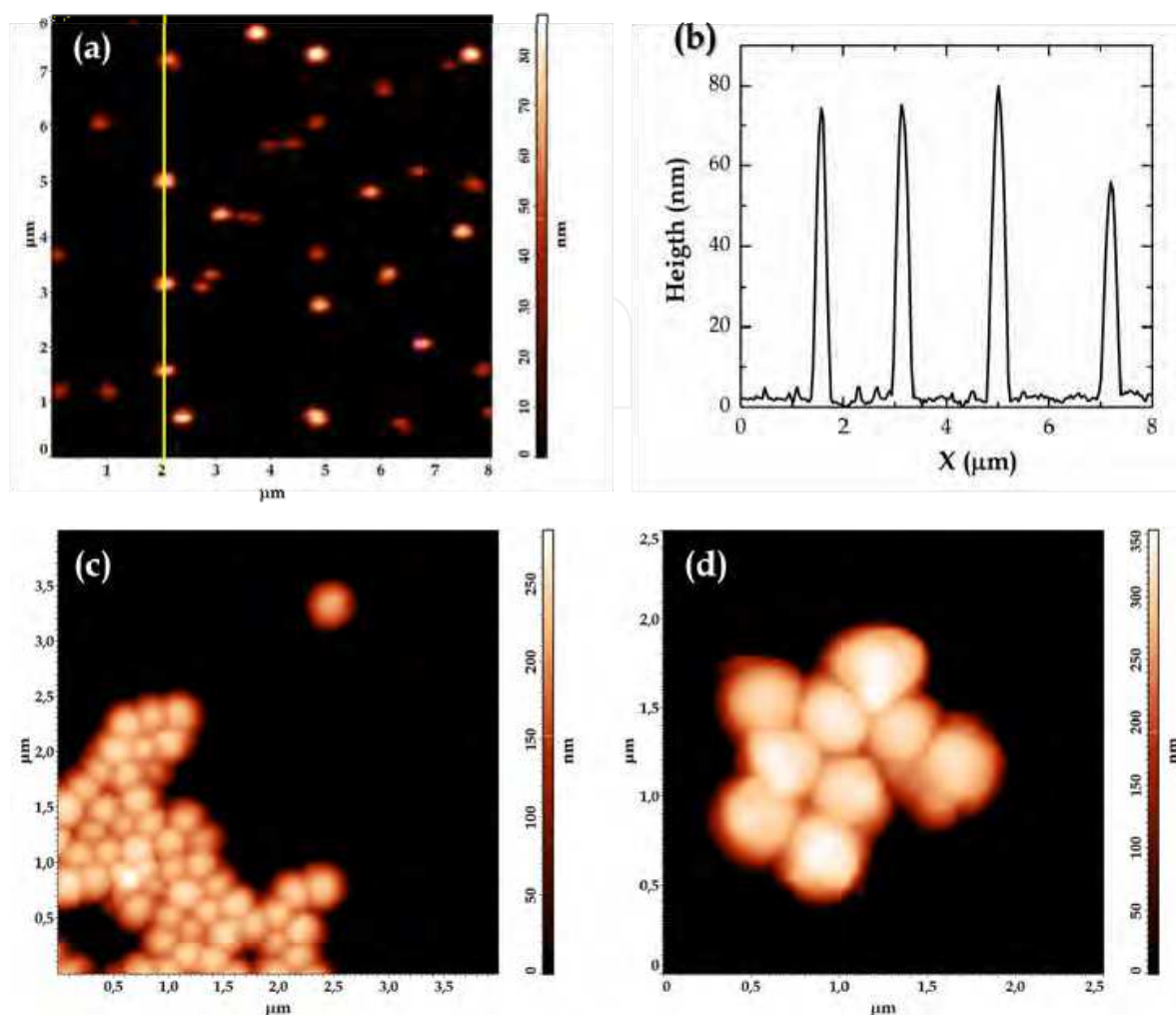


Fig. 3. (upper panel) AFM images in topography (a) and x-scan line (b) of void silica nanoparticles; (lower panel) AFM images in topography of fluorescein-functionalized silica nanoparticles (c) and void silica nanoparticles (d) in the presence of BSA.

collection which corresponds to the following 50% cut-point of 2.5 μm, 1.0 μm, 0.5 μm, 0.25 μm (filters A, B, C and D, respectively) on a 25 mm PTFE filter. The Impactor has a final step to collect the particles below the < 0.25 μm cut - point on a 37 mm PTFE filter (filter AF) equipped with a sample pump capable of maintaining a constant flow rate (about 9 l/min). For the morphological/dimensional characterization of the particulate through AFM imaging, the collected particulate was desorbed from the collection filters, since the latter presented a very rough surface which did not allow to have enough resolution. Each filter was transferred in 10 mL vials; in each vial 5 mL of water were added. The vials were then sealed and the desorption was carried out by ultrasonication for 20 minutes at room temperature. The morphological analysis was carried out upon deposition of the obtained suspensions on mica. The AFM images were collected in tapping mode in order to avoid sample degradation or removal. The AFM images show that the shape of the particulates formed is influenced by the nature of the working processes taking place during the sample collection, as well as the environmental conditions (temperature, pressure, material concentration). In particular, spherical objects were observed from the samples collected in places where digging process were carried out or where metals were treated at high temperatures, while the samples

collected in environments where blade are used (such as for wood processing) presented particles with quite sharp edges. Since the recent literature evidenced that the particle shape and size can affect their delivery and toxicity (Lewinski et al., 2008), the creation of a database containing the characterization of particulates produced in industrial working locations is particularly important to reduce the negative effects to personnel from exposure to these particulates within the working environment. Furthermore, the dimensional characterization has to be investigated in deeper details and AFM imaging provides a fast investigation tool which can give high resolution information. AFM topography images showed that the micron-size particulates collected in places where digging operations are carried out, or during metal processing, are constituted by smaller particles with dimensions between 15 and 100 nm. Even the samples desorbed from the collection filters with higher dimensional cut (Figure 4a, b and d) are constituted by smaller nanoparticles which form agglomerates with bigger dimensions. However, within the agglomerates, the nanostructure is maintained, as shown by the jagged linescan (Figure 4c) which presents steps about 25 nm height and can be attributed to the single nanoparticles composing the agglomerate.

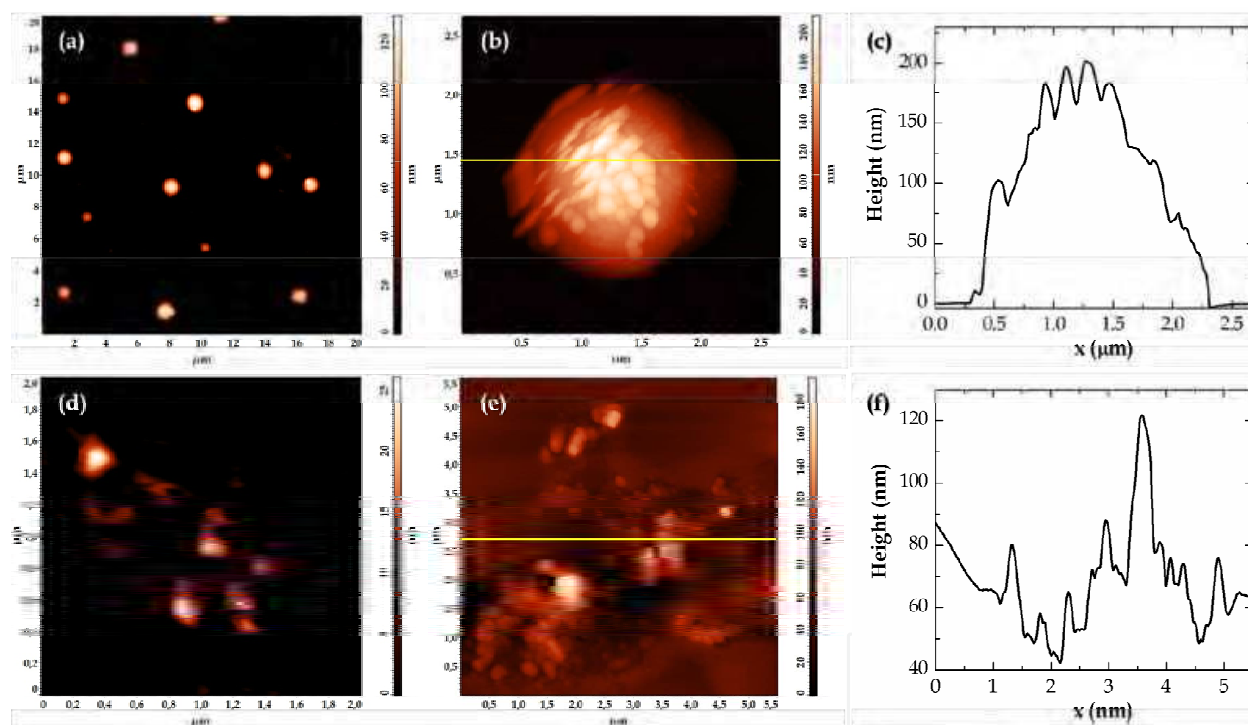


Fig. 4. (upper panel) AFM images representing the topography (a,b) and x-scan line (c) of nanoparticulate collected during digging operations (cut-off filter = 0.25  $\mu\text{m}$ ); (lower panel) AFM images representing the topography of nanoparticulate collected during metal welding operations (cut-off filter = 0.25  $\mu\text{m}$ ) in the absence (d) and in the presence of bacterial DNA (e) together with x-scan line graph (f) taken from the image (e).

## 2.2 Investigations of the interactions between nanoparticles and biomolecules

The interactions between colloidal nanoparticles and biomolecules were investigated by AFM through an analysis of the grain dimensions and morphology and the data in the absence of the biomolecules compared to those obtained in the presence of biomolecules.



Generally for all the colloidal nanoparticles under investigation, a marked increase in grain dimensions was observed upon interaction with protein or bacterial DNA. In particular gold nanoparticles bearing citrate ions on the surface interact efficiently with bacterial DNA. The interaction is so strong to be optically visualized by colour changes of the gold suspensions; the well known, intense red colour of gold suspensions turns to an intense blue upon addition of DNA (about  $10^{-4}$  M in base pair). This behaviour is obviously due to modifications of the Surface Plasmon Resonance (SPR) of the gold colloids, which is a deeply investigated phenomenon due to the potential application for sensing and labelling (Latterini & Tarpani, 2011). However, a much weaker effect can be observed when the single DNA base or mixtures of bases are added to gold colloids, thus the effect has to be related to DNA structure. AFM images recorded on gold-DNA complex deposited on mica (Figure 2e-f) show that the colloids are no longer detectable as individuals, but the samples are instead characterized by supramolecular architectures whose dimensions can reach the  $\mu\text{m}$  scale. This observation, together with the SPR shift to longer wavelength, suggested that DNA strands tend to accumulate around the metal particles likely replacing, at least in part, the citrate anions leading to micron-size aggregates formation. Inside these aggregates, gold colloids come into closer contact, as highlighted by the SPR shift, which is in agreement with literature data (Ghosh & Pal, 2007). The lack of clearly detecting the metal nanostructure even in phase mode is probably due to the fact that they are buried inside the biological layer which is estimated to be tens of nm thick if the average diameter of the pristine gold nanoparticles ( $12 \pm 0.3$  nm) is taken into account.

A similar aggregation phenomenon was observed also when bacterial or calf thymus DNA solutions were added to the suspensions of particulates collected from metal welding operations. In this case the metal nanoparticles are not intentionally prepared and stabilized thus interactions with DNA strands are enhanced to reach a better stabilization in the water media. As a results, particles with dimensions below 25 nm (Figure 4d) in the presence of DNA form aggregate structures with an overall dimension in the order of hundreds of nm.

A clustering effect was observed for silica nanoparticles when they were topographically imaged in the presence of Bovine Serum Albumine (BSA). In particular, the grain dimensions increased when the void silica nanoparticles were deposited in the presence of BSA; for 80 nm diameter particle, an increase by a factor of 4 was observed in the height and a larger effect was observed in the width (Figure 3d). These effects have been attributed to the adsorption of the protein on the surface of the silica nanoparticles, as previously observed for similar systems (Bellezza et al., 2009; Latterini & Amelia, 2009). Indeed, the net negative charge present on the void silica nanoparticles in aqueous neutral media can have an important role in controlling the adsorption of the protein which presents a positive net surface charge in the same pH conditions. This adsorption process resulted in a shielding effect from the negative charges which stabilized the naked particle and maintained isolation; thus the silica nanoparticles with BSA adsorbed on the surface tend to form clustered structures. However, no clear evidence was obtained by AFM to determine the conformation of the protein on the surface of the particles.

AFM can be also a valid means to study and comprehend the mechanism behind the interaction between organic nanomaterials and biomolecules. The protein Bovine Serum Albumin (BSA) is used as model biomolecule to investigate its interaction with polystyrene nanoparticles (PS NPs) synthesized in our group.

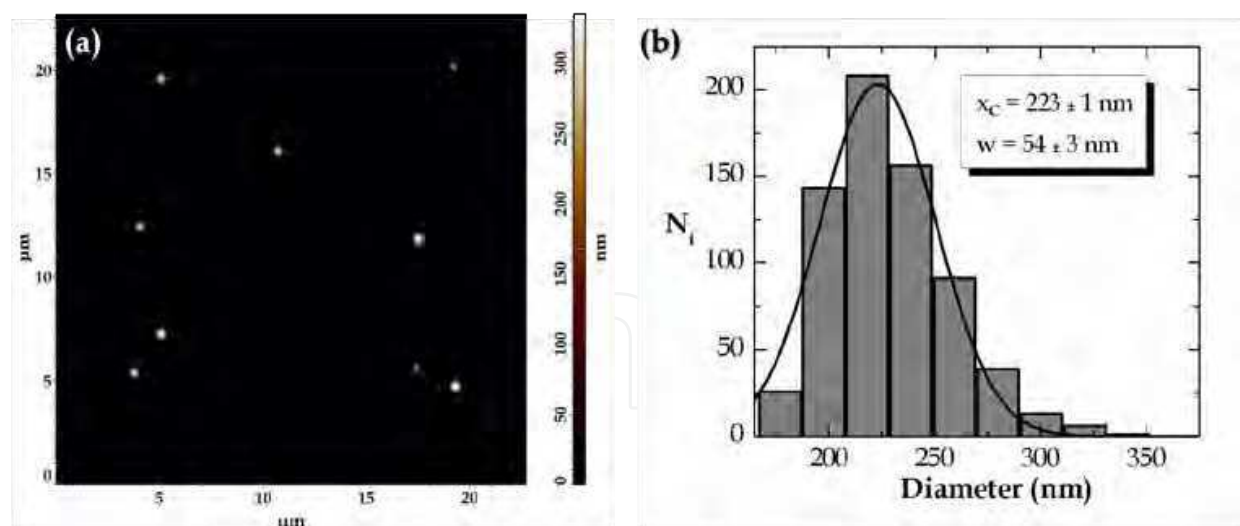


Fig. 5. AFM images representing the topography (a) of polystyrene NPs deposited on mica and relative size distribution built up from AFM images in (b).

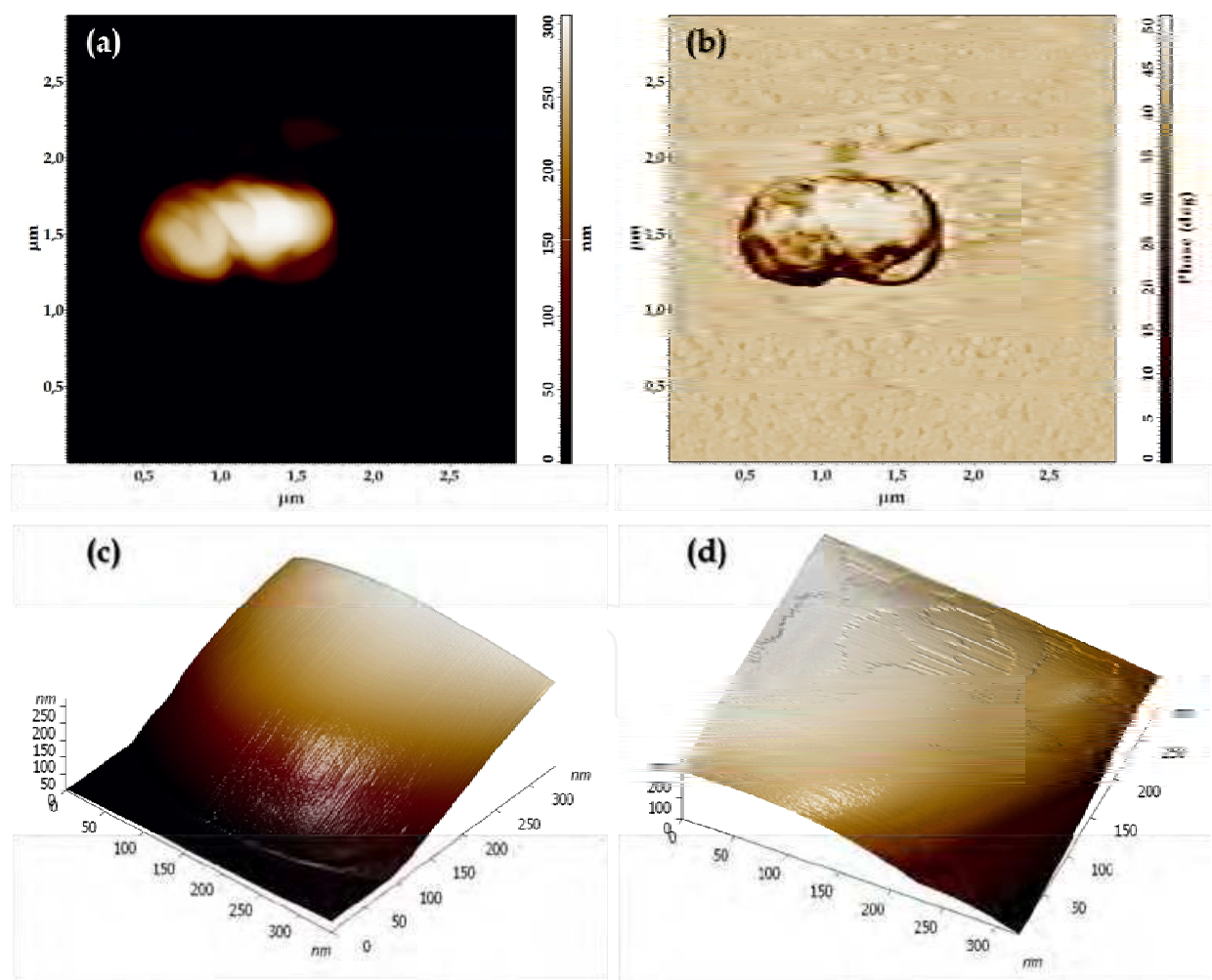


Fig. 6. (upper panel) AFM images representing the topography (a) and phase (b) of polystyrene NPs deposited on mica after BSA adsorption; (lower panel) 3-D AFM image of a polystyrene NP surface before (c) and after (d) BSA adsorption.

AFM topography images of a PS NPs sample deposited on mica by spin-coating demonstrate the presence of spherical particles with a smooth surface (Figure 5a). The height histogram built up from the AFM images (taking into account at least 500 particles) indicates that the nanoparticles are quite polydisperse with a mean diameter of about 230 nm (Figure 5b). A  $10^{-3}$  M aqueous solution of BSA was then added to the synthesized PS NPs and AFM topography images were collected after deposition on mica. Upon interaction with the protein, the images clearly show the formation of aggregates with an elongated shape but the same Z-height of the single nanoparticles (Figure 6a-b). The data seem to indicate that the adsorbed protein acts as a linker between the nanostructures binding them together in groups of three or four. It is known in literature (Yoon et al., 1996) that BSA can be adsorbed on a surface according to two different orientations: side-on, in which the longer side (14 nm) adheres to the surface or end-on, in which the shorter side (4 nm) is involved in the adsorption. A schematic representation of these two types of interaction is shown in Figure 7b. In this particular case, topography images in high resolution of the PS NPs surface were taken after BSA adsorption. The resulting 3-D topographic images demonstrate that upon interaction with BSA (Figure 6d) there is an increase of the surface roughness and the formation of a single protein layer adsorbed on the polystyrene nanoparticles. As shown by the x-scan profile (Figure 7a), this layer has a height of about 4 nm, thus confirming that BSA is adsorbed onto the polymeric NPs in the side-on orientation.

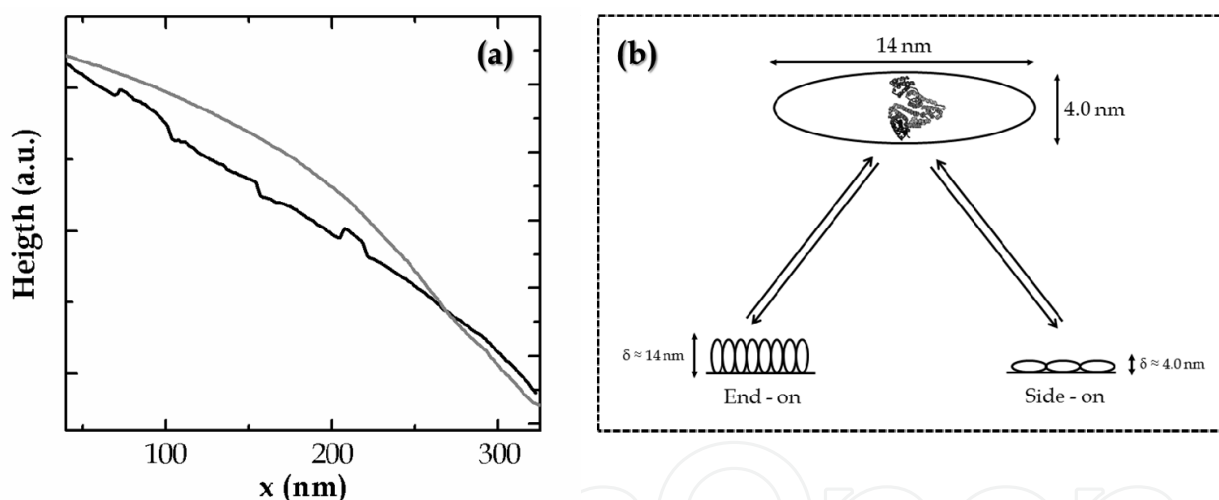


Fig. 7. (a) X-scan line graph of polystyrene NPs surface before (gray line) and after (black line) BSA adsorption; (b) Scheme of the possible orientations of BSA adsorbed on a solid surface

### 3. Conclusions

AFM scanning has been used to characterize, from a dimensional and morphological point of view, colloidal nanoparticles prepared intentionally with designed properties and particulates collected in working environments. The data obtained from AFM topography imaging, once statistically analyzed, were helpful to obtain information on the growth mechanism of CdS nanocrystals and gold nanoparticles. Indeed, a broadening of size distribution of CdS colloids suggested that the growth was mainly controlled by surface processes; on the other hand, the narrowing of dimensional populations for gold

nanoparticles indicated that the growth could occur through a diffusion controlled process. Interestingly, the comparison between topography and phase images allowed us to make the hypothesis that the stabilizer shell around the particles has a dimension of few nm thus colloidal nanoparticles can be better regarded as nanocomposites. Silica nanoparticles prepared through a sol-gel method were successfully imaged in topography mode and appeared well dispersed, with a narrow size distribution and a smooth surface.

AFM appears to be a valid tool also for a fast and high resolution analysis of particulates collected in working environments. Thus AFM imaging can be useful for the creation of a database on dimension and morphology of particulates produced in different working environments in order to evaluate their toxicity in relation to the tools and the conditions used. AFM topography images showed that the micron-size particulates collected in places where digging or welding operation are carried out are actually constituted by smaller particles with dimensions between 15 and 100 nm.

AFM is a valid mean to study and comprehend the interactions between nanomaterials and biomolecules. Generally for all the investigated nanoparticles, a marked increase in grain dimensions was observed upon interaction with protein or DNA. AFM images recorded on nanoparticle-biomolecule conjugates demonstrated that the effect is due to the formation of supramolecular architectures whose dimensions can reach the  $\mu\text{m}$  scale, in which electrostatic interactions might have an important role. Only in the case of polystyrene particles with 220 nm diameter, the BSA molecules adsorbed on their surface are arranged in an ordered conformation. The line-scan analysis through topographic images allowed us to establish the BSA orientation.

#### 4. Acknowledgment

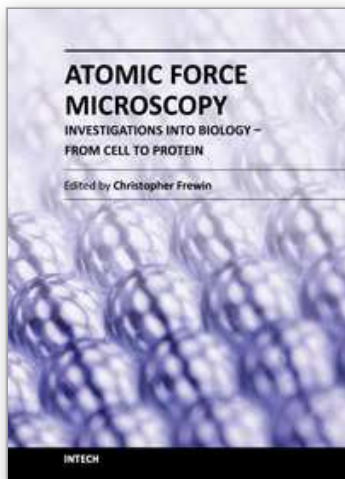
This work is supported both by the University of Perugia and the Department of the University for the Scientific and Technological Research (MIUR-Rome). Authors are grateful to INAIL for financial support through a research agreement (May 2010-2012) and for providing the samples collected in working environments.

#### 5. References

- Amelia, M.; Flamini, R.; Latterini L. (2010). Recovery of CdS nanocrystal defects through conjugation with proteins. *Langmuir*, Vol. 26, pp 10129-10134, ISSN 0743-7463
- Bellezza, F.; Cipiciani, A.; Latterini, L.; Posati, T.; Sassi, P. (2009). Structure and Catalytic Behaviour of Myoglobin adsorbed onto Nanosized Hydrotalcites. *Langmuir*, Vol. 25, pp 10918-10924, ISSN 0743-7463
- Dedecker, P.; Hotta, J.I.; Flors, C.; Sliwa, M.; Uji-I, H.; Roefsaers, M.B.J.; Ando, R.; Mizuno, H.; Miyawaki, A. & Hofkens, J. (2007). Subdiffraction imaging through the selective donut-mode depletion of thermally stable photoswitchable fluorophores: numerical analysis and application to the fluorescent protein Dronpa. *J. Am. Chem. Soc.*, Vol.129, No.51, (December 2007), pp. 16132-16141, ISSN 0002-7863
- García, R. & Pérez, R. (2002). Dynamic atomic force microscopy methods. *Surface Science Reports*, Vol.47, No.6-8, (April 2002), pp. 197-301, ISSN 0167-5729



- Ghosh, S.K. & Pal T., (2007). Interparticle coupling effect on the surface plasmon resonance of gold nanoparticles: from theory to applications. *Chem. Rev.*, Vol.107, No.11, , pp. 4797-4862, ISSN 0009-2665
- Hoo, C.M.; Starostin, N.; West, P.; Mecartney, M.L. (2008). A comparison of atomic force (AFM) and dynamic light scattering (DLS) methods to characterize nanoparticle size distributions, *J. Nanopart.Res.* Vol. 10, pp. 89-96.
- Irrgang, J.; Ksienczyk J.; Lapiene V. & Niemeyer C.M. (2009). Analysis of Non-Covalent Bioconjugation of Colloidal Nanoparticles by Means of Atomic Force Microscopy and Data Clustering. *ChemPhysChem*, Vol.10, No.9-10, (July 2009), pp. 1483-1491, ISSN 1439-4235
- Joralemon, M.J.; Smith, N.L.; Holowka, D.; Baird, B. & Wooley, K.L. (2005). Antigen-decorated shell cross-linked nanoparticles: Synthesis, characterization, and antibody interactions. *Bioconj. Chem.*, Vol.16, No.5, (September-October 2005), pp. 1246-1256, ISSN 1043-1802
- Knemeyer, J.P.; Marme, N. & Sauer, M. (2000). Probes for detection of specific DNA sequences at the single-molecule level. *Anal. Chem.*, Vol.72, No.16, (August 2000), pp. 3717-3724, ISSN 0003-2700
- Latterini, L.; Amelia, M., (2009). Sensing proteins with luminescent silica particles. *Langmuir*, Vol. 25, pp 4767–4773, ISSN 0743-7463
- Latterini, L. & Tarpani L. (2011). Hierarchical assembly of nanostructures to decouple fluorescence and photothermal effect. *J.Phys.Chem.C*, DOI: 10.1021/jp208124x, ISSN 1932-7455
- Lewinski, N. ; Colvin, V. & Drezek, R. (2008). Cytotoxicity of Nanoparticles, *Small*, Vol.4, No. 1, 26 – 49, ISSN 1613-6829
- Nehilla, B.J.; Vu, T.Q. & Desai, T.A. (2005). Stoichiometry-dependent formation of quantum dot-antibody bioconjugates: A complementary atomic force microscopy and agarose gel electrophoresis study. *J. Phys. Chem. B*, Vol.109, No.44, (November 2005), pp. 20724-20730, ISSN 1520-6106
- Passeri, R.; Aloisi, G.G.; Elisei, F.; Latterini, L.; Caronna, T.; Fontana, F. & Sora, I.N. (2009). Photophysical properties of N-alkylated azahelicene derivatives as DNA intercalators: counterion effects. *Photochem. Photobiol. Sci.*, Vol.8, No.11, (August 2009), pp. 1574-1582, ISSN 1474-905X
- Rosi, N.L. & Mirkin, C.A. (2005). Nanostructures in biodiagnostics. *Chem. Rev.*, Vol.105, No.4, (April 2005), pp. 1547-1562, ISSN 0009-2665
- Yoon, J.-Y.; Park, H.-Y.; Kim, J.-H.; Kim, W.-S. (1996), Adsorption of BSA on highly carboxylated microspheres-quantitative effects of surface functional groups and interaction forces *J. Colloid Interface Sci.*, Vol.177, 613-620, ISSN 0021-9797



## **Atomic Force Microscopy Investigations into Biology - From Cell to Protein**

Edited by Dr. Christopher Frewin

ISBN 978-953-51-0114-7

Hard cover, 354 pages

**Publisher** InTech

**Published online** 07, March, 2012

**Published in print edition** March, 2012

The atomic force microscope (AFM) has become one of the leading nanoscale measurement techniques for materials science since its creation in the 1980's, but has been gaining popularity in a seemingly unrelated field of science: biology. The AFM naturally lends itself to investigating the topological surfaces of biological objects, from whole cells to protein particulates, and can also be used to determine physical properties such as Young's modulus, stiffness, molecular bond strength, surface friction, and many more. One of the most important reasons for the rise of biological AFM is that you can measure materials within a physiologically relevant environment (i.e. liquids). This book is a collection of works beginning with an introduction to the AFM along with techniques and methods of sample preparation. Then the book displays current research covering subjects ranging from nano-particulates, proteins, DNA, viruses, cellular structures, and the characterization of living cells.

### **How to reference**

In order to correctly reference this scholarly work, feel free to copy and paste the following:

L. Latterini and L. Tarpani (2012). AFM Measurements to Investigate Particulates and Their Interactions with Biological Macromolecules, Atomic Force Microscopy Investigations into Biology - From Cell to Protein, Dr. Christopher Frewin (Ed.), ISBN: 978-953-51-0114-7, InTech, Available from:  
<http://www.intechopen.com/books/atomic-force-microscopy-investigations-into-biology-from-cell-to-protein/afm-measurements-to-investigate-particulates-and-their-interactions-with-biological-macromolecules->

**INTECH**  
open science | open minds

### **InTech Europe**

University Campus STeP Ri  
Slavka Krautzeka 83/A  
51000 Rijeka, Croatia  
Phone: +385 (51) 770 447  
Fax: +385 (51) 686 166  
[www.intechopen.com](http://www.intechopen.com)

### **InTech China**

Unit 405, Office Block, Hotel Equatorial Shanghai  
No.65, Yan An Road (West), Shanghai, 200040, China  
中国上海市延安西路65号上海国际贵都大饭店办公楼405单元  
Phone: +86-21-62489820  
Fax: +86-21-62489821

© 2012 The Author(s). Licensee IntechOpen. This is an open access article distributed under the terms of the [Creative Commons Attribution 3.0 License](https://creativecommons.org/licenses/by/3.0/), which permits unrestricted use, distribution, and reproduction in any medium, provided the original work is properly cited.

IntechOpen

IntechOpen